THESIS FOR THE DEGREE OF DOCTOR OF PHILOSOPHY

Distributed Multi-Antenna Systems using 1-bit Radio-over-Fiber.

Lise Aabel

Department of Electrical Engineering
Chalmers University of Technology
Gothenburg, Sweden, 2025

Distributed Multi-Antenna Systems using 1-bit Radio-over-Fiber.

Lise Aabel
ISBN 978-91-8103-277-2

Acknowledgements, dedications, and similar personal statements in this thesis, reflect the author's own views.

Doktorsavhandlingar vid Chalmers tekniska högskola
Ny serie nr 5735
ISSN 0346-718X

Department of Electrical Engineering
Chalmers University of Technology
SE-412 96 Gothenburg, Sweden
Phone: +46 (0)31 772 1000

This work was supported in part by the Swedish Foundation for Strategic Research under Grant ID19-0036 and in part by the Sweden's Innovation Agency under Grant 2024-02404.

Cover:
A distributed multi-antenna system transmitting cooperatively to two user terminals.

Printed by Chalmers Digital Printing
Gothenburg, Sweden, August 2025

Distributed Multi-Antenna Systems using 1-bit Radio-over-Fiber.

Lise Aabel
Department of Electrical Engineering
Chalmers University of Technology

Abstract

Distributed multiple-input multiple-output (D-MIMO) is a promising approach to improve the wireless mobile network coverage and meet increasing capacity demands. Its foundation builds upon the ability to cooperatively utilize spatially distributed radio access nodes to exploit macro diversity. However, in order to implement spatial multiplexing, precise phase coherence at carrier frequency is required across all cooperating radio nodes. This poses a challenging implementation problem, since a radio typically uses a local oscillator to generate the carrier frequency, and each local oscillator is associated with a frequency offset and phase noise. In this thesis, we propose a D-MIMO architecture that eliminates local oscillators at the radio heads altogether, and implements instead digital frequency up- and down-conversion in a central processing unit, such that the radio frequency signals are phase-synchronized at the remote radio heads. This architecture relies on fiber-optic fronthaul, over which 1-bit signals are transferred.

First, we introduce a D-MIMO transceiver architecture that employs 1-bit quantization to reduce power consumption and facilitate efficient fiber-optic fronthaul. Phase-coherence is demonstrated in a wireless multi-user measurement implementing reciprocity-based precoding. Second, since this architecture relies on significant oversampling to battle the distortion introduced by the 1-bit converters, we investigate the tradeoff between oversampling in the spatial or temporal domain, when the total fronthaul rate is constrained. This sheds light on the minimum fronthaul rate required in a certain deployment for our D-MIMO architecture to outperform standard co-located MIMO architecture. Third, we present a testbed that we use to investigate the receiver architecture effects on multi-user scenarios. We find that our architecture shows greater uplink sensitivity to multi-user interference than a conventional receiver, and that user power control can mitigate this sensitivity.

Keywords: D-MIMO, Radio-over-Fiber, 1-bit converter

In honour of my parents.

List of Publications

This thesis is based on the following publications:

[A] **Lise Aabel**, Sven Jacobsson, Mikael Coldrey, Frida Olofsson, Giuseppe Durisi, Christian Fager, "A TDD Distributed MIMO Testbed Using a 1-Bit Radio-Over-Fiber Fronthaul Architecture". Published in IEEE Transactions on Microwave Theory and Techniques, Vol. 72, No. 10, Oct. 2024.

[B] Anzhong Hu, **Lise Aabel**, Giuseppe Durisi, Sven Jacobsson, Mikael Coldrey, Christian Fager, Christoph Studer, "EVM Analysis of Distributed Massive MIMO with 1-Bit Radio-over-Fiber Fronthaul". Published in IEEE Transactions on Communications, Vol. 72, No. 11, Nov. 2024.

[C] **Lise Aabel**, Giuseppe Durisi, Mikael Coldrey, Frida Olofsson, Christian Fager, "Insights on the Uplink Operation of a 1-bit Radio-over-Fiber Architecture in Multi-User D-MIMO Communication". Submitted to IEEE Transactions on Microwave Theory and Techniques.

Other publications by the author, not included in this thesis, are:

[D] S. Jacobsson, **L. Aabel**, M. Coldrey, I. C. Sezgin, C. Fager, G. Durisi and C. Studer, "Massive MU-MIMO-OFDM uplink with direct RF-sampling and 1-bit ADCs". *IEEE Globecom Workshops*, Waikoloa, HI, USA, Dec. 2019.

[E] **L. Aabel**, G. Durisi, I. C. Sezgin, S. Jacobsson, C. Fager and M. Coldrey, "Distributed massive MIMO via all-digital radio over fiber". *Proc. 54th Asilomar Conf. Signals, Syst., and Comput.*, Pacific Grove, CA, USA, Nov. 2020.

[F] I. C. Sezgin, **L. Aabel**, S. Jacobsson, G. Durisi, Z. S. He and C. Fager, "All-digital, radio-over-fiber, communication link architecture for time-division duplex distributed antenna systems". *J. Lightw. Technol.*, Vol. 39, No. 9, pp. 2769–2779, May, 2021.

[G] F. Olofsson, **L. Aabel**, M. Karlsson and C. Fager, "Comparison of transmitter nonlinearity impairments in externally modulated sigma-delta-over fiber

vs analog radio-over-fiber links". *Proc. Opt. Fiber Commun. Conf. (OFC)*, San Diego, CA, USA, Mar. 2022.

[H] A. Bordbar, **L. Aabel**, C. Häger, C. Fager and G. Durisi, "Deep-learning-based channel estimation for distributed MIMO with 1-bit radio-over-fiber fronthaul". *19th Int. Symp. Wireless Commun. Syst. (ISWCS)*, Rio de Janeiro, Brazil, Jul. 2024.

[I] S. Jacobsson, **L. Aabel**, I. C. Sezgin, C. Fager and M. Coldrey, "Radio transceiver device configured for dithering of a received signal". Eur. Patent EP3991307, Feb. 2025.

[J] F. Olofsson, **L. Aabel**, T. Eriksson, M. Karlsson and C. Fager, "Sigma-delta-over-fiber with WDM serial connection for distributed MIMO". *J. Lightw. Technol.*, Vol. 43, No. 5, pp. 2151–2162, Mar., 2025.

[K] F. Olofsson, C. Lim, K. Lee, M. Karlsson, **L. Aabel**, T. Eriksson, and C. Fager, "Demonstration of multi-user distributed MIMO at mm-wave using sigma-delta-over-fiber and optical up-conversion". Submitted to J. Lightw. Technol.

Contents

Acknowledgments

After finishing my master's degree, my then-manager Adjunct Professor Mikael Coldrey gave me the opportunity to work toward a PhD degree at Ericsson Research. By some, this academic path is referred to as "the golden ticket". I was of course extremely flattered and honored, but I remember signing the contract with a little disclaimer "just be aware that I am not sure I want to do this". One might think that this comment is a sign of ungratefulness, but I did not see it that way. I believe that I speak for (almost) all researchers when I say that when we do something, we do it with full dedication. Promising an extreme effort for five years should, perhaps, come with a disclaimer. Countless hours in the lab, deep in thought while cycling up and down the hill to Chalmers campus, here we are, five years later. And the road has been bumpy. Pursuing a doctoral degree has truly been a ride of self-development, and a test of patience and resilience. But one thing is for certain: I would never have completed this journey without all of the support I have received along the road.

First of all, I would like to thank Mikael Coldrey for seeing my potential and believing in me. Thank you for finding me worthy of the golden ticket. Next, I would like to thank my supervisors, Professor Christian Fager and Professor Giuseppe Durisi. Learning from your brilliant minds, in two different disciplines, has taught me invaluable skills that I will carry with me for the rest of my life. Thank you for teaching me structure, thoroughness, to question my results, and for trusting me. I believe that our project has taught us all a lot. Thank you Doctor Sven Jacobsson, for your positivity and expertise, and for always finding the time to help me. On this journey, I have had the pleasure of learning from so many extremely talented people I extend my deepest gratitude to all of my collaborators and colleagues for the inspiring discussions, the fun, and the unwavering support. I would also like to direct my gratitude to everyone at the Microwave Electronics Laboratory at MC2 for respecting my signs on the door. Thank you also to everyone in the Communication Systems Group at E2 for always making me feel welcome. The same goes for everyone at Ericsson Research at Lindholmen—I'm truly excited and proud to soon be working with all of you "for real". Working across three organizations has been both challenging and rewarding, and I am grateful to have been part of such talented communities. A special thank you goes to my dear friend and work-wife Frida Olofsson, for keeping me sane

through the ups and downs, for endless discussions, and for always being in the mood for coffee.

Perhaps most importantly, I dedicate this final paragraph to everyone in my life who does not have interest in the contents of this thesis. Without my family and friends, this would have been a hollow experience. To my mother, my late father, and my brothers: thank you for always thinking highly of me, no matter what I do for work. To Lisa, Danira, and Hanna: thank you for always making me laugh. And to my beloved Stina, thank you for the tremendous love and support. You make me calm and happy, even in the darkest of times.

Acronyms

ADC:	Analog-to-Digital Converter
AGC:	Automatic Gain Control
BBU:	Baseband Unit
BS:	Base Station
CU:	Central Unit
DAC:	Digital-to-Analog Converter
DC:	Direct Current
DU:	Distributed Unit
(e)CPRI:	(evolved) Common Public Radio Interface
EVM:	Error-Vector Magnitude
FPGA:	Field-Programmable Gate Array
IF:	Intermediate Frequency
LNA:	Low-Noise Amplifier

LO:	Local Oscillator
MIMO:	Multiple-Input-Multiple-Output
OFDM:	Orthogonal Frequency-Division Multiplexing
PA:	Power Amplifier
PAM:	Pulse-Amplitude Modulation
QAM:	Quadrature Amplitude Modulation
RF:	Radio Frequency
RU:	Radio Unit
RRH:	Remote Radio Head
SFP:	Small Form-factor Pluggable
SNR:	Signal-to-Noise Ratio
TDD:	Time-Division Duplex
UE:	User Equipment
VGA:	Variable Gain Amplifier

Part I

Overview

CHAPTER 1

Introduction

1.1 Background

Mobile telecommunication technology has revolutionized the way in which we communicate. Today, there are 8.7 billion mobile subscriptions worldwide, and the forecast for 2030 is 9.5 billion [1]. This vast usage of mobile devices puts high expectations on the reliability and quality of service of the wireless network. Users expect reliable service to, e.g., buy a bus ticket, order food, live-stream meetings, and make payments. Beyond everyday applications, wireless networks shall also be able to support advanced use cases, such as industrial automation, autonomous driving, and joint communication and sensing. These applications require ultra-reliable communication, low latency, and tight synchronization, which further complicates the network design. To accommodate the ever-increasing demands on the communication capacity and performance, a new generation of the cellular network has been launched every decade (most recently 5G, in 2019). Figure 1.1 illustrates the distribution of mobile subscriptions across different technologies. Historically, users have consistently migrated to newer network platforms, and forecasts predict that by 2030, 80% of the global mobile traffic will be carried by the

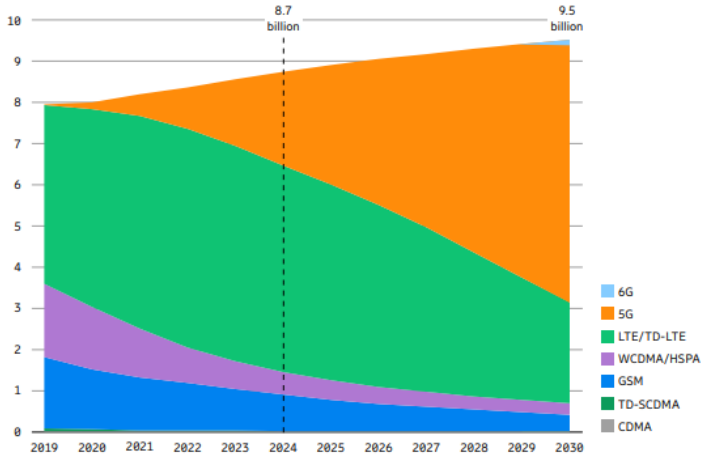

Figure 1.1. Mobile subscriptions by technology (billion) [1].

5G network. This trend underscores the market's attraction to the enhanced performance delivered by each technological advancement. Looking ahead, the anticipated launch of 6G in 2030 promises unprecedented capacity and capabilities, setting the stage for further innovation.

Each generation of the wireless network spurs the growth of unforeseen business opportunities and network applications. Therefore, the telecommunication network needs to evolve in symbiosis with emerging businesses and societal needs. To enable new services and applications, innovative technical solutions and comprehensive standardization are essential. Capacity-enhancing functionalities and advancements are incorporated into the network standards to become part of the next generation network platform. Currently, we find ourselves in the transition between 5G and the 6G release, and the new network requirements are being formulated. According to forecasts, seamless handovers, minimized energy usage, and high reliability are among the top priorities for 6G network technology [1].

For a mobile device to establish a wireless connection to the internet, it transmits and receives signals via a radio base station, which serves as an interface between the mobile device and the broader network infrastructure. The radio base station is allocated a specific bandwidth over which electromagnetic waves carrying information are transmitted. By facilitating wireless

transmission and reception of signals, the radio base station serves both as a critical bottleneck and a key enabler in connecting users to the internet. Its capabilities thus directly influence the network's capacity, coverage, and overall performance. As the network grows, advancements in radio base station technology are therefore essential. Since the 3G release, the multiple-input multiple-output (MIMO) antenna system has been a cornerstone in advancing the radio technology. A MIMO system builds upon using multiple transmit and receive chains in the radio [2]. Directional transmission and reception of electromagnetic waves is then enabled, commonly known as beamforming. By focusing the transmitted signals in a certain direction, the signal-to-noise ratio (SNR) is increased. This enables a reduction in transmit power, and thus improves the energy efficiency. Furthermore, by observing a signal on multiple antennas, the spatial diversity makes the reception more resilient to fluctuations in the signal strength [3]. Beamforming also enables spatial multiplexing, which means that multiple user equipments (UEs) in a cell can communicate on the same time-frequency resources if they are spatially separable. Increasing the number of antennas (or radio chains) in the MIMO antenna system improves further the capacity, coverage, and UE throughput, which has taken the MIMO technology into the paradigm of massive MIMO, involving hundreds of antennas within the radio base station [2].

However, despite all the benefits that MIMO technology offers, a fundamental challenge in MIMO systems is to battle wireless channel fading due to changes in the surrounding environment [4]. When objects move, they alter how electromagnetic waves scatter, leading to random fluctuations in the signal strength at the receiver. Each radio chain has its own wireless channel to the UE, and if the fading among the channels are correlated—meaning the signal strength drops simultaneously across the multiple channels—it becomes difficult to overcome the negative impact on communication performance. To address this, techniques that improve the diversity among the channels can be used. One effective method is to place the antennas far apart, which makes it less likely that the fading will be correlated across the channels. Consequently, at least some channels will exhibit good channel conditions with high probability [5]. Distributed (D)-MIMO refers to an architectural framework that utilizes multiple geographically dispersed antennas to serve UEs in a cooperative manner [4], [6]. The significance of a D-MIMO system lies in its potential to enhance both coverage, capacity, and energy efficiency, while

enabling more flexible and scalable network designs. By leveraging the inherent diversity across channels, D-MIMO can outperform conventional MIMO systems. D-MIMO networks have been popular in the research community for a long time under various terminologies, including cell-free MIMO, centralized radio-access network (C-RAN), distributed antenna systems (DAS), heterogenous networks (HetNets), and coordinated multi-point (CoMP). In fact, CoMP has been incorporated into the 3GPP standard since 2013 [7]. However, commercial D-MIMO systems are still not widely available on the market, primarily because very tight synchronization is required among all cooperating nodes, which can be costly and is challenging to achieve. In this thesis, we explore a cost-effective D-MIMO architecture that achieves by design synchronization among all distributed nodes.

1.2 Thesis outline

This thesis is divided into two parts. Part I serves as an introduction to Part II, which consists of the papers. The remainder of Part I is organized as follows. Chapter 2 gives a brief introduction to multi-user MIMO communication. In Chapter 3, an overview of the wireless network infrastructure is provided, and different approaches to build D-MIMO wireless networks are discussed. The D-MIMO architecture that is studied in this thesis is motivated in Chapter 4. Chapter 5 discusses other successful approaches that have demonstrated multi-user D-MIMO. A summary of the papers that constitutes this thesis is given in Chapter 6, followed by concluding remarks and future research directions in Chapter 7.

CHAPTER 2

Fundamentals of Multi-User MIMO

Regardless of the specific network architecture, in a multi-user MIMO system, multiple antennas at the network base station (BS) enable simultaneous data transmission to and from several UEs. This chapter offers a high-level introduction to multi-user MIMO communication. Specifically, this thesis examines a wireless system that uses time-division duplex (TDD) technology, where transmission and reception of wireless signals occur in the same frequency band but at different scheduled times [2, Ch. 2]. The communication frame is thus divided into time slots, dedicated for either uplink (from UE to the network) or downlink (from the network to the UE). This approach enables dynamic adjustment of uplink and downlink traffic loads and simplifies the hardware design by using a single frequency band.

The uplink and downlink signals in the multi-user MIMO system are exchanged between the BS and UE antennas over the air, which constitutes the wireless channel. Figure 2.1 illustrates a MIMO system with $B = 3$ BS antennas and $U = 2$ single-antenna UEs. Each complex scalar element h_{bu} represents the channel between BS antenna b and UE u, describing how the signal's amplitude and phase are altered as the signal passes through the channel. The whole channel is typically represented by the channel matrix

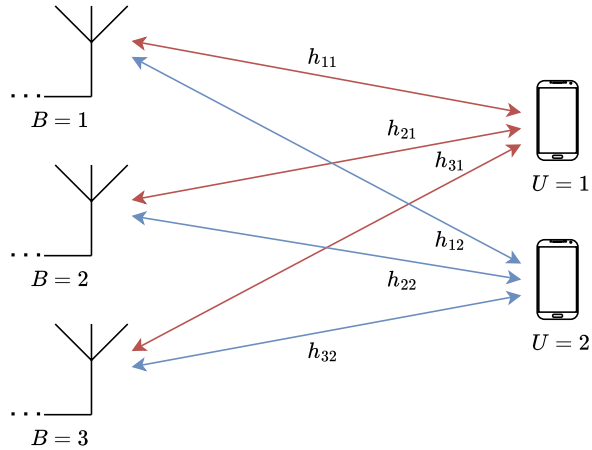

Figure 2.1. Multi-user MIMO in a 3×2 setup.

$\mathbf{H} \in \mathbb{C}^{B \times U}$. This channel can be characterized either by its impulse response or frequency response. The received signal in the uplink of this system can be modelled at the discrete time instance n as

$$\mathbf{y}_n^{\mathrm{UL}} = \mathbf{H}\mathbf{s}_n^{\mathrm{UL}} + \mathbf{w}_n, \tag{2.1}$$

where $\mathbf{s}_n^{\mathrm{UL}} \in \mathbb{C}^U$ denotes the signals transmitted by the U UEs, and $\mathbf{w}_n$ represents Gaussian noise. Similarly, the downlink model becomes

$$\mathbf{y}_n^{\mathrm{DL}} = \mathbf{H}^{\mathrm{T}}\mathbf{u}_n + \mathbf{w}_n, \tag{2.2}$$

where $\mathbf{u}_n \in \mathbb{C}^B$ denotes the signals transmitted by the B BS antennas.

By estimating the channel matrix, the effects of the channel can be effectively mitigated in both the uplink and downlink. In the uplink, the U signals received across the B antennas are *combined* using the estimated channel information. This combining process coherently aligns the incoming signals from each user, improving signal quality and enabling accurate demodulation. In the downlink, the transmit signals are *precoded* based on the channel matrix. Precoding adjusts the amplitude and phase at each transmit antenna element,

enhancing the signal strength towards intended users while minimizing interference to others. Consequently, a multi-user MIMO system enables spatial multiplexing, allowing multiple data streams to be transmitted simultaneously over the channel.

The example in Figure 2.1 involves three BS antennas that transmit and receive two data streams, one per user. By constructing a combining matrix $\mathbf{W} \in \mathbb{C}^{U \times B}$ and a precoding matrix $\mathbf{P} \in \mathbb{C}^{B \times U}$, the BS can process the user data streams $\mathbf{s}_n^{\mathrm{UL}}$ and $\mathbf{s}_n^{\mathrm{DL}} \in \mathbb{C}^U$ such that

$$\mathbf{r}_n = \mathbf{W}\mathbf{y}_n^{\mathrm{UL}} \tag{2.3}$$

and

$$\mathbf{u}_n = \mathbf{P}\mathbf{s}_n^{\mathrm{DL}}. \tag{2.4}$$

The matrices $\mathbf{W}$ and $\mathbf{P}$ are designed based on the estimated channel matrix $\widehat{\mathbf{H}}$ to maximize signal quality while minimizing inter-user interference. Common strategies include zero-forcing (ZF), minimum mean square error (MMSE), and maximum ratio (MR) [2, Ch. 3]. These techniques differ in their trade-offs between complexity, interference mitigation, and noise enhancement. Through effective combining and precoding, multi-user MIMO systems can significantly increase spectral efficiency and system capacity by serving multiple users simultaneously on the same time-frequency resources.

The necessity of combining and precoding highlights the importance of channel estimation in MIMO systems. However, the wireless channel varies over both time and frequency, which requires frequent channel estimation over the signal bandwidth. The channel is typically decomposed into short time intervals and fractional bandwidths, in which the channel is assumed to be static. The channels must be estimated and used for precoding within this short time interval before it is outdated. Frequent channel estimation is performed by transmitting known sequences, called pilots, which are used to infer the channel characteristics.

Specifically in TDD systems, since the transmitter and receiver use the same frequency band, channel reciprocity can be exploited. This concept builds upon that the wireless channel's propagation characteristics are the same in the uplink and the downlink, as modelled in (2.1) and (2.2). As a result, the BS can derive the downlink channel state information from the uplink channel estimate. This allows the precoder to be computed from the

uplink estimate, facilitating adaptive and dynamic precoding. This approach is efficient because it eliminates the need for feedback of the channel state information from the UE. However, although the wireless channel itself is reciprocal, the effective channel includes hardware components in both the UE and the BS, through which the signals pass. Such analog signal processing introduces amplitude- and phase shifts, and nonlinear effects. The models presented in (2.1) and (2.2) are therefore naïve, and do not consider that the components that process the signals in the uplink and downlink are different. In reality, the effective uplink and downlink channels are not reciprocal, and the system requires reciprocity calibration. In fact, to utilize the wireless channel reciprocity, calibration of the transmitter and receiver is necessary.

Note that a TDD system can also utilize the downlink channel estimates. In this case, the UEs estimate the channel based on downlink pilots and feed this information back to the BS for scheduling and precoding. Since the BS usually transmits at higher power than the UE, the downlink SNR is generally higher, leading to a better quality channel estimate [3, Ch. 3]. Nevertheless, feeding back the estimate increases uplink traffic load. In a D-MIMO system, exploiting reciprocity is even more beneficial than in a co-located MIMO system. This is because downlink channel estimation requires coordinated transmission from all involved antennas in the network, which can be costly in terms of signaling resources. Best practices in channel state information acquisition are thus nontrivial, and require dynamic trade-off evaluation.

CHAPTER 3

Distributed MIMO Architectures

In a multi-user D-MIMO network, the B antenna terminals are spatially dispersed rather than co-located at a single BS. This spatial distribution introduces unique challenges and requirements for channel estimation and precoding compared to traditional MIMO systems with centralized antennas. The objective of this chapter is to investigate the various design strategies and architectural options for constructing an efficient D-MIMO network. Throughout this exploration, we will uncover how each design choice introduces complexities across different system domains.

3.1 Network Building Blocks

Let us begin by examining the building blocks of the conventional wireless network infrastructure. The radio access network for 4G and 5G technology is constructed by the block diagrams presented in Figure 3.1 [8]. The "Core" represents the part of the network that manages data routing and connection to the internet. In 4G, the core network connects via backhaul to a baseband unit (BBU), which is the bridge between the radio and the core. Most of the digital signal processing is executed in the BBU, including signal modulation

and demodulation, MIMO processing, and higher layer protocols. The BBU is often placed in a more convenient location than a radio tower, and connects to a remote radio head (RRH) via fronthaul, which carries digital baseband data. All analog signal processing is performed in the RRH, including sampling, frequency conversion, and amplification. One could say that the BBU is the brains and the RRH is the muscle, and together they make a radio BS. The fronthaul is commonly an optical fiber cable connection, operated using the digital (enhanced) common public radio interface (eCPRI) packet-based standard [9].

In 5G, to increase network adaptability, a new terminology was introduced to divide the BBU into several logic nodes; the central unit (CU), the distributed unit (DU), and the radio unit (RU). The split between the digital functions assigned to the logical nodes is flexible and is commonly known as the functional split [10]. Note that, even with the functional split that assigns the fewest tasks to the RU (option 8), the RU performs the analog signal processing and is equipped with a digital block to convert signals between the digital fronthaul interface and the radio front-end. Despite the difference in terminology, both the RRH and RU are responsible for radio frequency (RF) front-end processing. In this thesis, we explore a cellular D-MIMO system in which we refer to a number of RRHs, connected to one common CU. In the subsequent chapters, we provide a detailed examination of the roles and interactions of these two nodes within the proposed architecture.

Figure 3.2 compares the conventional cellular MIMO concept, in which all antenna elements are co-located at a radio BS, with the D-MIMO cellular architecture, in which the antenna elements are distributed among multiple RRHs. The illustrated scenario involves a UE that is subject to shadowing by a blocking building in the conventional cellular MIMO network. On the contrary, the geographical advantage of the RRHs in the D-MIMO network prevents shadowing, since the UE is observed by the network from multiple points in space. By proper coordination by the CU, the transmitted signals from multiple RRHs can be aimed at the same UE. Similarly, in the uplink, signals can be received on multiple RRHs and combined at the CU. This type of network coordination is why D-MIMO offers very high reliability. Furthermore, the more dense the D-MIMO network, the closer will the UE be to at least a few the RRHs. This closeness translates to low path loss, which increases the SNR. One can use this benefit to lower the transmit power from

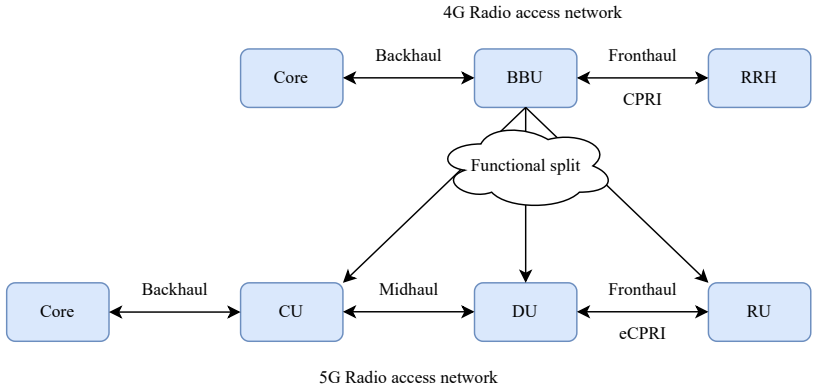

Figure 3.1. The 4G and 5G radio access network structure.

both the RRHs and UEs, and increase energy efficiency.

It becomes clear that the network architectures illustrated in Figure 3.2 are subject to different requirements. In the co-located MIMO network, the operational decision making is executed within the BS, but in the D-MIMO network, to facilitate that the RRHs cooperatively serve the UEs in the cell, it is required that the CU coordinates the network. The CU must gather real-time information from all RRHs to make informed decisions and allocate resources efficiently. To facilitate this process, dedicated fronthaul links between the CU and the RRHs are advantageous. These can essentially be either wireless or wired connections, but fiber-optic fronthaul presents an excellent option due to the high reliability, low loss, and substantial capacity they offer. The CU can in principle implement various cooperation schemes among the RRHs, each imposing different design requirements on the system. The choice of cooperation scheme reflects a trade-off between implementation complexity, resource demands, and achievable performance gains. One approach is RRH selection, where only the RRH that offers the best performance for each UE is utilized [11]. This method minimizes coordination overhead and complexity, but does not utilize the system resources effectively, and in order to achieve uninterrupted connectivity, seamless handovers are required. Alternatively, the network can employ a time-interleaving scheme, in which multiple RRHs

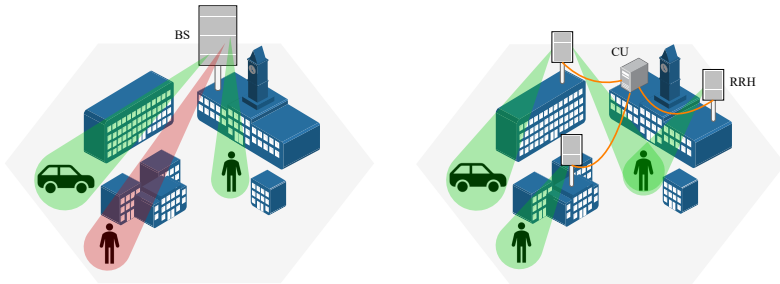

(a) (b)

Figure 3.2. Network concept for (a) co-located MIMO and (b) distributed MIMO.

transmit to a UE at different times [12]. This approach can improve the coverage and reliability, although it requires precise frame synchronization and may introduce latency. The most ambitious and capacity-enhancing approach is coherent joint transmission, where all RRHs simultaneously transmit to the UEs [4]. This approach facilitates distributed beamforming, leveraging the combined resources of all RRHs to significantly improve signal quality and system throughput. However, it demands synchronization in time, frequency, and especially RF phase alignment, resulting in considerable implementation challenges. We shall in the following section pinpoint the difficulties in implementing a D-MIMO network using conventional radio design, and discuss possible solutions.

3.2 The Radio Front-End

Transmission and reception of wireless signals require efficient conversion between analog RF electromagnetic waves and digital information signals. This process is handled by the radio front-end, which involves analog signal processing tasks such as filtering, amplification, and frequency conversion, which are performed by microwave components. These tasks are assigned to the RRH, which implements the necessary microwave circuitry. On the other hand, digital signal processing tasks include modulation and demodulation, channel estimation, precoding, combining, and equalization, and are performed by a processor. These tasks are generally distributed between the RRH and the

CU [10].

The Conventional Radio Transceiver

Figure 3.3 illustrates the fundamental components of a conventional radio transceiver architecture. The block on the right represents the digital signal processing tasks including signal modulation and demodulation. To the left of the digital domain is the radio front-end, with the uppermost pathway representing the transmitter chain. In the transmitter, source data intended for a UE is first modulated into complex-valued symbols, typically using a QAM constellation map. These symbols undergo orthogonal frequency-division multiplexing (OFDM) modulation, where they are assigned to orthogonal subcarriers and converted to the time domain. Alternatively, pulse shaping filters may be applied to limit the signal bandwidth and reduce inter-symbol interference. The in-phase (I) and quadrature (Q) components of the resulting signals are generated by a pair of digital-to-analog converters (DACs), producing the analog baseband signal. This baseband signal contains all the information within the designated bandwidth of the system, and is centered at zero or low frequency. To up-convert the baseband signal to the carrier frequency, the I and Q components are combined and mixed with a frequency tone generated by a local oscillator (LO). The resulting RF signal is then amplified and transmitted through the antenna port. On the receiving side, the RF signal is first amplified by a low-noise amplifier (LNA) to compensate for path loss. The amplified signal is then down-converted to intermediate frequency (IF) or baseband using a mixer. Finally, a pair of analog-to-digital converters (ADCs) sample and quantize the baseband signals, enabling subsequent demodulation and signal processing to be performed digitally.

The primary role of the ADC is to transform the continuous-time, analog signal into a discrete-time, digital signal. This involves sampling the signal at a specific rate and quantizing its amplitude levels. The resolution of the ADC, determined by its number of bits, defines the number of discrete amplitude levels that can be represented, while the sampling rate, determined by the clock, decides the maximum frequency that can be accurately captured [13, Ch. 2]. Conversely, DACs perform the reverse operation, translating digital signals into analog waveforms. Typically, both ADCs and DACs operate at baseband frequencies–low enough to reduce complexity, cost, and power consumption–rather than directly at RF. This approach is advanta-

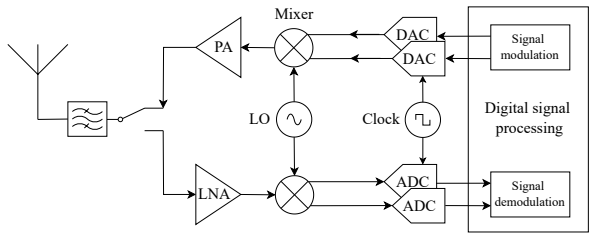

Figure 3.3. The conventional transceiver.

geous because the power consumption of data converters increases with both the sampling rate and the resolution. Theoretically, the power consumption of an ADC increases linearly with sampling rate and exponentially with resolution [14]. The empirical study of different ADC technologies in [15] shows that the power exceeds a linear increment as a function of the sampling rate, making low-rate operation more practical for wireless transceivers.

The mixers in Figure 3.3 are four-port devices that produce at the output the sum and difference of its input signals, enabling frequency translation between RF and baseband. They rely on the LO to produce as an input signal a stable tone that determines the carrier frequency. To ensure high signal integrity and meet stringent performance requirements, the LO must exhibit excellent frequency stability, tunability, and low phase noise. However, in practical implementations, the LO is subject to frequency instability, known as phase noise, which causes spectral spreading and degrades the signal quality [16].

To transmit phase-coherent signals in a D-MIMO system using a conventional transceiver architecture, the geographically dispersed LOs must be synchronized. However, each LO inherently exhibits its own phase noise and frequency offset, which will lead to inaccurate beamforming. For effective coherent joint transmission among the RRHs, it is essential that all LOs are precisely synchronized and phase-locked. Achieving such synchronization across widely distributed LOs is technically challenging and significantly increases the system complexity, potentially rendering impractical implementations [17]. Practical solutions to LO synchronization in D-MIMO is discussed in Chapter 5.

The Direct RF-Sampling Radio Transceiver

To avoid the complexities associated with synchronizing LOs across distributed RRHs, we consider an alternative approach. Although high-resolution and high-speed converters typically consume significant energy, imagine a system where the RF signal is sampled directly without the need for mixers. In this architecture, up- and down-conversion are performed entirely in the digital domain, eliminating the need for mixers altogether. An illustration of this direct RF-sampling transceiver is shown in Fig. 3.4. While this design simplifies the RF front-end compared to a conventional transceiver, it shifts the complexity to the ADCs and DACs, which must handle high sampling rates and resolution. To fulfill the Nyquist rate, the sampling rate must be at least

$$f_s \geq 2f_c + W, \tag{3.1}$$

where f_c is the carrier frequency and W is the signal bandwidth. Consequently, a large number of samples must be processed digitally.

The elimination of mixers and LOs in the transceiver architecture makes the direct RF-sampling approach particularly attractive for D-MIMO systems [18]. However, in a multi-antenna system, many RF chains are required, each equipped with a pair of DAC and ADC. As the number of chains increases, the power consumption of high-speed, high-resolution ADCs and DACs becomes a significant concern. To address this, low-resolution converters have gained popularity in direct RF-sampling transceivers [19]–[22]. By reducing the resolution, the overall power consumption can be minimized, making the architecture more practical for large-scale implementations. From the perspective of D-MIMO networks, this solution circumvents the problem of synchronizing distributed LOs and keeps at the same time the power consumption of the converters at a minimum. Because of these benefits, the D-MIMO architecture explored in this thesis involves direct RF-sampling with low resolution converters. We will now discuss how such a system can be implemented in the context of a CU interconnected with fronthaul to several RRHs.

3.3 The Fronthaul

In commercial radio access networks, digital radio signals are transferred over fiber-optic fronthaul using standardized protocols such as CPRI and eCPRI.

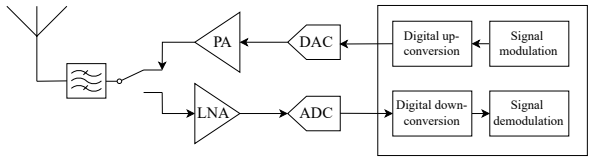

Figure 3.4. The direct RF-sampling transceiver.

These protocols define the interface and data transport methods between the DU and RU, enabling flexible deployment of network infrastructure. The process of transmitting radio signals over fiber-optic cables is collectively known as *radio-over-fiber*, which leverages the low loss and high bandwidth capabilities of optical fibers to carry signals over long distances. Note that this section discusses radio-over-fiber technology in the context of direct RF-sampling transceivers for the purpose of implementing D-MIMO. However, radio-over-fiber technology is versatile and can be adapted for many other applications, with various deployment architectures and configurations possible depending on the use case and system requirements.

Digitized Radio-over-Fiber

Digitized radio-over-fiber is the dominating fronthaul technology used in commercial systems, and the CPRI/eCPRI belongs to this category. In this approach, the RF signals are digitized and exchanged as digital bit streams between the RRHs and the CU. Figure 3.5 illustrates the digitized radio-over-fiber architecture, in which the RRH is equipped with ADC and DAC to convert between the analog and digital domains [23]. The electrical-to-optical (E/O) and optical-to-electrical (O/E) transceivers utilize binary transmission, making them relatively simple and cost-effective hardware components. In fact, these optical transceivers belong to the family of small form-factor pluggable (SFP), which are available as high-speed devices. Their widespread use in, e.g., data centers has accelerated technology development, resulting in robust and economical solutions. Furthermore, binary optical pulses are robust to non-linear effects in the optical domain, which minimizes signal distortion [24], [25].

However, to build a D-MIMO network based on digitized radio-over-fiber, despite the absence of the mixer and local oscillator, synchronization is re-

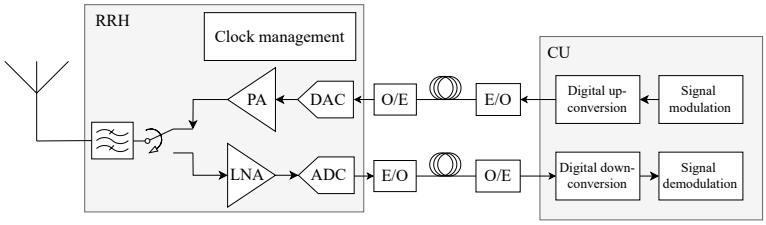

Figure 3.5. Digitized Radio-over-Fiber.

quired among the RRHs. The reason is that both the DAC and ADC rely on a clock, which will require timing and frequency synchronization across the entire network to incorporate accurate joint beamforming. As will be discussed in Chapter 5, this synchronization can be achieved by distributing a common clock to all RRHs over the fronthaul. The RRHs will, however, require complex hardware to accommodate the data converters and clock mechanisms, which halts the system scalability.

Analog Radio-over-Fiber

To mitigate the complications of implementing DACs and ADCs in the RRHs, analog radio-over-fiber can be used [26], [27]. In this approach, the RF signal is directly modulated onto an optical carrier without prior digitization, meaning that the DACs and ADCs are only required at the CU. This architecture is depicted in Figure 3.6. The figure shows a significantly simplified RRH design, and clock management in the RRH is not needed. The E/O transmitters in this design modulate the RF waveform onto the optical carrier. At the RRH, only amplifiers and filters are required in the RF path, which makes the RRH purely analog and simple by design.

While this method reduces complexity in the RRH and avoids synchronization issues, the optical waveform is susceptible to optical nonlinearities and noise, which degrades the signal quality [24], [25]. This method thus trades the complexity of implementing ADCs and DACs in the RRHs for complexity in the optical domain [28].

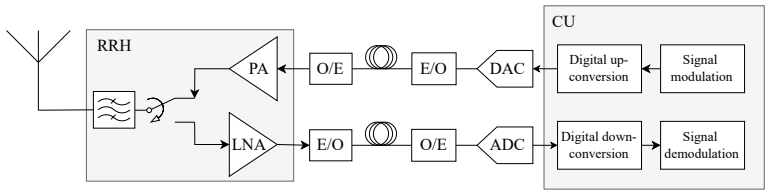

Figure 3.6. Analog Radio-over-Fiber.

Sigma-Delta-over-Fiber

Sigma-delta-over-fiber has been shown as an approach to leverage the robustness of binary optical transmission, while maintaining the simplicity of the RRH architecture [29]. This technique builds on the sigma-delta modulator, that converts a high-resolution signal into a lower-resolution format [30], [31]. Here, the input to the sigma-delta modulator is the high-resolution RF signal, and the output is a 1-bit representation of that signal. In general, reducing the amplitude resolution of a signal introduces quantization noise, which can lead to significant signal distortion within the bandwidth of interest. However, sigma-delta modulation mitigates this issue by employing oversampling and noise-shaping techniques. These methods shift the majority of the quantization noise outside of the bandwidth of interest, such that an analog filter can reconstruct the high-resolution signal without significant distortion. Consequently, low-resolution DACs, when coupled with careful filtering, can be used to generate high-resolution signals with this technique. The sigma-delta modulator is discussed in more detail in Section 4.2.

In the sigma-delta-over-fiber architecture, depicted in Figure 3.7, the RF signals are converted into 1-bit representation, enabling the use of digital optical transceivers for the fronthaul link. This architecture centralizes the computational operations in downlink signal generation, and simplifies the RRH downlink path to consist only of a reconstructive bandpass filter and a power amplifier (PA). However, implementing the uplink path is more challenging, as sigma-delta modulation must occur in the RRH. Like the DAC and ADC, the sigma-delta modulator requires a clock. Therefore, also this architecture relies on clock synchronization in the uplink path.

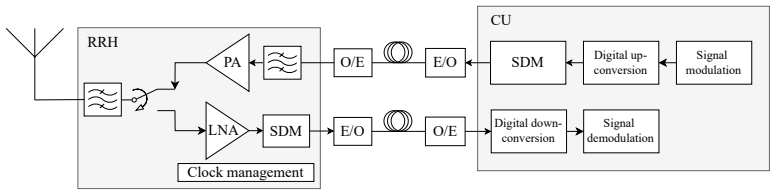

Figure 3.7. Sigma-Delta-over-Fiber.

3.4 The Central Unit

In a D-MIMO network, the CU serves as the central processing hub that manages and coordinates the operations of multiple RRHs. In fact, the CU must be able to aggregate the signals from multiple RRHs to act as a single coordinated multi-antenna system. This coordination enables the network to leverage spatial diversity and improve communication performance through techniques such as beamforming and interference management. In the context of the direct RF-sampling transceiver, the CU assumes additional responsibilities, including digital up- and down-conversion. This adds complexity to the processing tasks and imposes stringent requirements on both the computational power and the capability to perform real-time signal processing. The Nyquist sampling criterion, as expressed in (3.1), introduces a significant oversampling factor to accurately generate and sample the RF signals. Consequently, the CU must handle and process a vast volume of samples, which further intensifies the demand for efficient processing algorithms and high-performance hardware to ensure seamless network operation.

Furthermore, this work focuses on a network implementing coherent joint transmission, which means that the RRHs transmit signals simultaneously to the UEs. To ensure that these transmissions combine constructively at the UEs, the CU must maintain precise timing synchronization across all channels. This strict timing alignment is essential for achieving coherent combining gains, which significantly enhance the overall network performance. The key motivation of sampling directly at RF is to circumvent the complexity and challenges associated with synchronizing LOs distributed across the RRHs. The phase stability across channels is instead ensured by employing a shared LO located centrally within in the CU. This allows the system to maintain a consistent phase reference, which significantly simplifies the hardware design

of the RRHs and enhances system robustness against phase noise and drift. These promises rely solely on an accurate clock network in the CU.

To be able to exploit the reciprocity of the wireless channel, the CU must be able to estimate the channel in the uplink phase and use this channel estimate for downlink precoding. Achieving this requires not only maintaining precise phase stability among the various communication channels, but also ensuring that this phase coherence is preserved across both the transmitting and receiving paths. In other words, the CU must ensure that the phase references remain consistent when switching between uplink reception and downlink transmission. This dual-path phase stability is essential because any phase drift or mismatch can degrade the accuracy of the channel reciprocity assumption, leading to suboptimal precoding and reduced network performance.

CHAPTER 4

The 1-bit Radio-over-Fiber Fronthaul Architecture

Neither the digitized radio-over-fiber nor the sigma-delta-over-fiber fronthaul techniques provide a simple RRH design in the uplink because clock synchronization among the RRHs is required. Meanwhile, analog radio-over-fiber suffers from optical nonlinear distortion and attenuation. In order to keep the RRH hardware implementation simple, and at the same time avoid comprehensive clock management, quantization of the received signal by means of a comparator at the RRH has been proposed [32]–[35]. In this uplink architecture, the comparator converts the RF signal into a binary format without involving a clock, and the resulting signal is transferred using optical transmission to the CU, where it is sampled. This architecture ensures that the RRH design remains simple, and that clock management among the RRHs is avoided. Papers A–C investigate a D-MIMO architecture, chosen for its inherent phase stability and scalability, that implements sigma-delta-over-fiber in the downlink and quantization by means of a comparator in the RRH in the uplink, as shown in Figure 4.1. This architecture uses a binary, or 1-bit, representation of the RF signals to leverage fiber-optic fronthaul transfer using on-off intensity modulation. In this chapter, we discuss how this 1-bit quantizing architecture can be used to keep the signal distortion low.

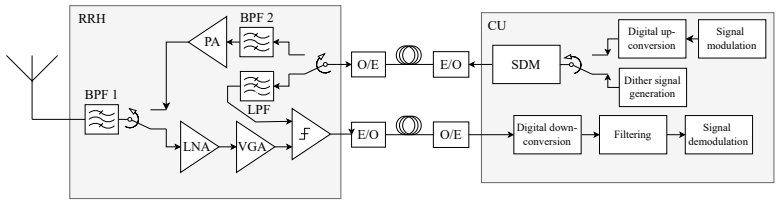

Figure 4.1. The 1-bit radio-over-fiber architecture.

4.1 Quantization Distortion

Quantization of a signal involves mapping of its continuous amplitude values into a finite set of discrete levels. The quantizer's objective is to produce an output signal that closely resembles the original input signal, despite being restricted to a limited number of amplitude levels. If the number of quantization levels are few, as is the case with few-bit quantizers, the resulting quantization error—the difference between the original and quantized signals—can be significant. This error manifests as quantization noise, which not only reduces signal fidelity but can also be correlated with the signal itself, thereby causing nonlinear distortion.

To illustrate quantization distortion in relation to the resolution of the quantizer, Figure 4.2 depicts a signal that is quantized by a 3-bit and a 1-bit quantizer. Specifically, it depicts a continuous sinusoidal input signal (shown in black), its quantized version (shown in blue), and the quantization error (in red). The quantization error in noticeably larger for the 1-bit quantizer, which is the most extreme case of amplitude discretization: the signal can only take two levels. Such coarse quantization introduces the largest possible quantization error, severely degrading the quality of the reconstructed signal due to the distortion.

Our D-MIMO architecture implements 1-bit quantization in both the uplink and the downlink path. To capitalize on the technical simplicity of the RRH and fronthaul, it is necessary to efficiently minimize the distortion introduced by the 1-bit quantization. Without effective distortion mitigation, the system's overall performance and spectral efficiency would suffer. To address this challenge, our architecture incorporates sigma-delta modulation in the downlink and dithering in the uplink. Sigma-delta modulation shapes the quantization noise spectrum, pushing the noise power out of the band-

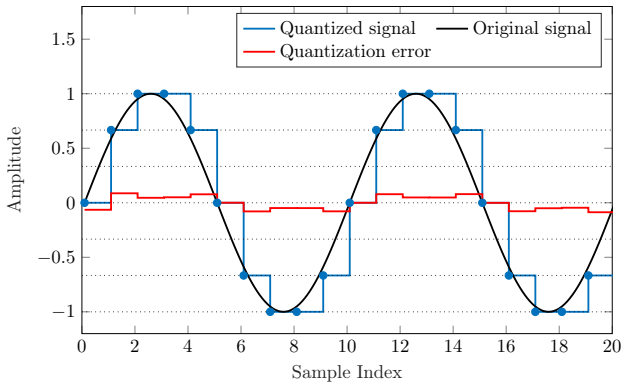

(a) 3-bit quantization

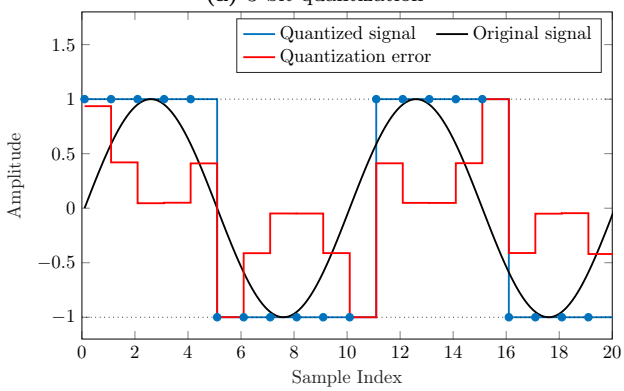

(b) 1-bit quantization

Figure 4.2. Signals before and after quantization.

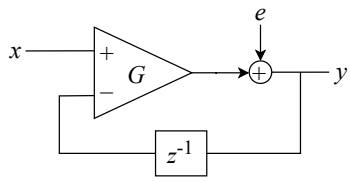

Figure 4.3. Quantizer with feedback.

width of interest, while dithering adds a controlled form of noise to decorrelate the quantization noise from the signal to reduce distortion. Together with oversampling, these methods enable the network to harness the benefits of 1-bit-resolution quantizers.

4.2 Sigma-Delta-over-Fiber Downlink

The uppermost chain of blocks in Figure 4.1 marks the downlink path, describing the same sigma-delta-over-fiber based architecture presented in Section 3.3. The signal modulation block involves the conversion from an information carrying bitstream into the baseband signal aimed for the RRH. This signal is up-sampled and up-converted to carrier frequency in the digital domain, and fed to a bandpass sigma-delta modulator, which converts the high-resolution bandpass signal into a 1-bit representation of that signal. The signal is, in this process, shaped in such a way that the quantization distortion is focused outside of the signal bandwidth of interest. This is made possible by high oversampling and noise-shaping.

To gain a deeper understanding of how a sigma-delta modulator works, let us take a moment to examine the simple circuit presented in Figure 4.3 [31]. In this circuit, an input signal x is fed to the input port of an amplifier with gain G. At the output of the amplifier, an error term e is added to the signal, resulting in the output signal y. This output signal is then fed back with a one-sample delay, denoted in the z-domain by z^{-1}, to the negative input port of the amplifier. In the context of our quantizing circuit, the error term e represents the quantization error. In terms of z-transforms—an effective tool to analyze circuits in discrete-time—the output signal y is described by

$$\begin{aligned} Y(z) &= (X(z) - z^{-1}Y(z))G + E(z) \\ &= \frac{G}{1+Gz^{-1}}X(z) + \frac{1}{1+Gz^{-1}}E(z), \end{aligned} \tag{4.1}$$

where we can separately identify the signal transfer function and noise transfer function as the terms in front of $X(z)$ and $E(z)$. To make sure that our circuit remains stable, we must identify the poles in the z-plane of this discrete-time system. The poles are defined by the root of the denominator of the system, namely $z = -G$. To make this system stable, it is required that $G < 1$. However, our goal is to design a circuit that minimizes the quantization error, which can only be done by making G large. In fact, we observe that the noise term vanishes only when $G \to \infty$. It is thus not possible to null the distortion with this system. The solution is to make G frequency dependent, and allow G to be large only for a small part of the total bandwidth. If the input signal x occupies only a small part of the total system bandwidth, that signal will then suffer only from minimal distortion when quantized by the system. Only under these circumstances can the system be stable and at the same time minimize the distortion on the signal x; the distortion cannot vanish but only be focused on certain frequencies. By introducing oversampling, the total bandwidth can be made large, such that the fraction of the bandwidth that is occupied by the input signal—in which we wish to minimize the signal distortion—is small in comparison. Oversampling is thus a key component when quantizing a signal with this system.

The sigma-delta modulator is built upon this concept, and implements instead of the constant gain G an integrator, which is a system that provides frequency dependent gain. Although the distortion within a fraction of the total bandwidth can be minimized, it cannot be made equal to zero over the full fractional bandwidth. To further battle the in-band distortion, sigma-delta modulators are generally much more complicated than the example circuit in Figure 4.3. Several integrators with negative feedback can be cascaded, which will shape the distortion to become even more focused outside of the bandwidth of the input signal. The number of cascaded integrators in a sigma-delta modulator is referred to as the *order* of the modulator.

To optimize the performance of a sigma-delta modulator, we investigate the expression for its dynamic range (DR), which can be approximated as

$$\mathrm{DR} \approx 6.02 \cdot B + 1.76 + 10 \log_{10} \left((2L+1) \cdot \mathrm{OSR}^{2L+1} / \pi^{2L} \right), \tag{4.2}$$

where B is the number of bits of the modulator, L is the order of the modulator, and OSR is the oversampling ratio defined as $\mathrm{OSR} = f_s/(2W)$, where f_s is the sample rate and W is the signal bandwidth [36]. Specifically, we are concerned with using $B = 1$ in the 1-bit radio-over-fiber architecture. This leaves the parameters L and OSR to optimize the dynamic range of the sigma-delta modulator. The number of cascaded integrators, L, decides the total transfer function of the system, and thereby how well we can suppress the noise within the bandwidth of interest. Importantly, the order of the sigma-delta modulator must be carefully chosen not to violate the stability of the system [31, Ch. 4]. Equation (4.2) tells us that the dynamic range is decided by striking a balance between the OSR and L.

In the 1-bit radio-over-fiber system, the sigma-delta modulator is applied to the RF signal in the downlink. This requires bandpass sigma-delta modulation, that nulls the quantization noise at the carrier frequency. The modulator is then designed to have a resonating behavior rather than a low-pass integrating behavior [31, Ch. 11]. Since the quantization noise is placed outside the bandwidth of interest, it is of utmost importance that it can be suppressed well enough by a bandpass filter such that it is not transmitted at the antenna port. Otherwise, this noise will generate adjacent channel leakage and cause interference in other bands. It is therefore important to consider the shape of the quantization noise in symbiosis with the bandpass filter that shall suppress it.

Hardware implementations

To operate the sigma-delta-over-fiber downlink in real-time, it is essential that the sigma-delta modulator located at the CU is realized in a digital circuit. This is typically achieved through hardware platforms such as an application-specific integrated circuit (ASIC) or a field-programmable gate array (FPGA). For development purposes, the FPGA serves as an excellent experimental platform due to its re-programmability and flexibility. There is a substantial body of research demonstrating the successful implementation of sigma-delta modulators on FPGAs, see, e.g., [37]–[40]. These studies provide a strong foundation and reference points for ongoing development in this area.

Notably, recent advancements have pushed the boundaries of performance and capability. For example, the implementation reported in [38] showcases a sigma modulator capable of efficiently handling a signal bandwidth up to 1 GHz, which is significant for high-speed communication applications.

Additionally, other studies have expanded the modulator's functionality to support carrier aggregation, as demonstrated in [41]. This capability is crucial to combine multiple frequency bands to increase the data throughput. Furthermore, the work in [39] demonstrates 60 dB adjacent channel leakage ratio, highlighting the ability to minimize interference with neighboring channels, despite the noise-shaping. Together, these developments illustrate the practical viability and evolving sophistication of sigma-delta modulators implemented on digital platforms.

4.3 1-bit Radio-over-Fiber Uplink

In the uplink path in Figure 4.1, denoted by the lower block chain, the RF signal is received at the antenna port at the RRH and passed through a bandpass filter and a LNA. The output of the LNA is fed to an amplifier with automatic gain control (AGC) that adjusts its gain to convert the signal power to a certain range. The signal is then fed to the comparator, which quantizes the input signal to two levels. During the uplink stage, the CU is generating simultaneously a *dither signal* that is sent to the RRH via the downlink optical fronthaul. This dither signal is sigma-delta modulated at the CU and low-pass filtered at the RRH to suppress the quantization noise. It is then fed to the second port of the comparator. The comparator quantizes the difference between the RF signal and the dither signal. The comparator outputs a high or low voltage of amplitude A according to

$$V_{\text{out}} = \begin{cases} A, & V_{\text{in}+} > V_{\text{in}-} \\ -A, & V_{\text{in}+} < V_{\text{in}-}, \end{cases} \tag{4.3}$$

where the input signals to the differential ports of the comparator, $V_{\text{in}+}$ and $V_{\text{in}-}$, denote the instantaneous RF signal and dither signal voltages, respectively. The output voltage of the comparator modulates a laser that transfers the binary signal to the CU, where it is sampled. It may seem counterintuitive to deliberately add a dither signal prior to the quantizer, we shall therefore now discuss the dithering process.

Dithering

Dithering is a common technique used in analog-to-digital conversion to reduce the correlation between the quantization error and the input signal [42]. It involves adding a signal, called the dither, to the signal before quantization. The dither signal is typically a noise term, with the purpose to influence the decision of the quantizer. As a result, the quantization noise becomes more randomized, or whitened, and can be effectively reduced through filtering, which improves the signal quality. To establish some intuition about dithering, consider the signals shown in Figure 4.4, which illustrate the signals before and after quantization. Unlike Figure 4.2, the original signals (in black) include added Gaussian noise. When the quantizer maps the continuous signals to discrete amplitude levels, the added noise affects its decisions, causing the quantization error (in red) to exhibit a more random behavior, as depicted in the figure. This randomness, together with oversampling, whitens the quantization error such that it becomes less correlated with the signal.

From the analysis of Figure 4.2, we observe that decreasing the quantizer's resolution leads to an increase in quantization error. Consequently, a stronger dither signal is needed to sufficiently randomize this error. However, if the dither signal becomes too strong, it can overwhelm the original signal with excessive noise, degrading the signal quality. This trade-off implies the existence of an optimal dither signal power that balances effective error randomization without significantly compromising the integrity of the desired signal.

Although noise signals are commonly used as dithering signals, there are no established guidelines for the optimal shape of the dithering signal in our 1-bit radio-over-fiber architecture. Since a relatively strong dithering signal is necessary to effectively randomize the quantization error when using a 1-bit quantizer, noise may not be the most suitable choice. Similar to the approach used in sigma-delta modulators, we aim to generate a binary signal that carries our RF signal with minimal distortion. This concept is widely applied in other domains as well. For example, pulse width modulation is a method in which an analog signal is converted into a pulse train with varying pulse widths, which can then be filtered to reconstruct the original analog signal [43]. In pulse width modulation, the amplitude of the analog signal directly determines the duration of each pulse. Compared to sigma-delta modulation, pulse width modulation does not rely on feedback, and is simpler to implement. A common approach in, e.g., power conversion and fiber-optics, involves quantizing the

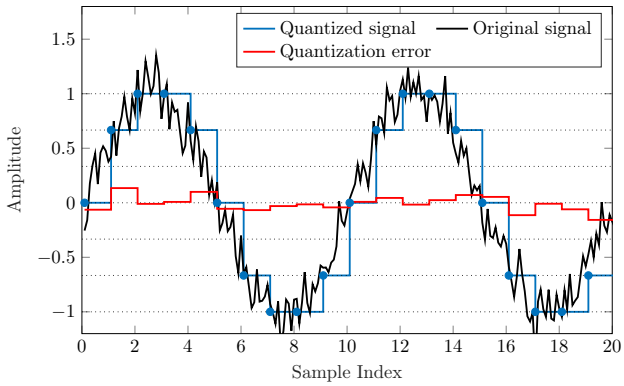

(a) 3-Bit quantization with 13 dB SNR.

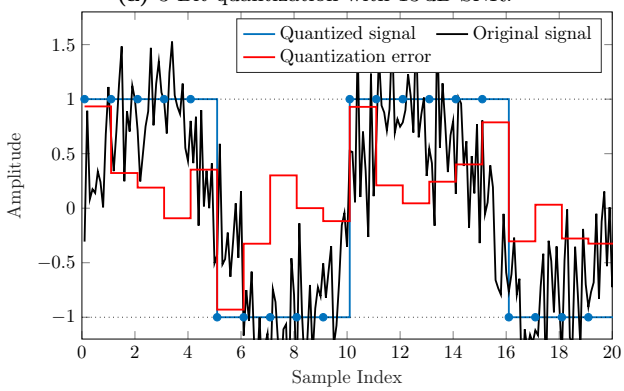

(b) 1-Bit quantization with 5 dB SNR.

Figure 4.4. Quantization of a sinusoid with Gaussian dither.

difference between the analog signal and a triangular waveform [44], [45]. This triangular signal serves then as a dithering signal. By carefully designing the triangular waveform, the correlation between the quantization error and the input signal can be significantly reduced [37].

When the difference between the information signal and the triangular dither signal is quantized, the resulting output frequency spectrum exhibits sidebands at multiples of the triangular signal's frequency [46]. To prevent these sidebands from interfering with the signal bandwidth of interest, the frequency of the triangular dither signal should be approximately on the order of the information signal's bandwidth [37]. The amplitude of the dithering signal also plays an essential role; it must be large enough to keep the signal distortion to a minimum. Therefore, the dither amplitude should be carefully optimized based on the characteristics of the information signal, making it inherently dependent on the signal properties.

To illustrate this technique, we present in Figure 4.5(a) the input and output signals of a 1-bit quantizer. In this example, the information signal is a RF waveform with 75 MHz bandwidth, modulated onto a 2 GHz carrier. The triangular dither signal has a frequency of 110 MHz, which is sufficient to avoid overlap with the signal bandwidth. Investigations of optimal dither frequency are presented in Paper A. In Figure 4.5(a), we observe that the quantized signal exhibits more fluctuations when the RF signal amplitude is large, and longer pulses when it is small. This indicates how the information in the RF signal is contained in the quantized signal. Figure 4.5(b) compares the spectrum of the quantized RF signal with and without triangular dithering. Without dithering, severe signal distortion is indicated by the broadened signal bandwidth. When dithering is applied, the signal distortion is significantly reduced, though sidebands appear at predictable locations determined by the dither frequency.

Oversampling

According to the Nyquist theorem, to reconstruct an analog signal in discrete-time, the sample rate must be at least twice as large as the highest frequency component of the analog signal. However, in our 1-bit quantizing receiver with dithering, the system relies on significant oversampling beyond this minimum rate. Increasing the sampling rate improves the time resolution, which captures more details in the signal. Intuitively, this oversampling has an av-

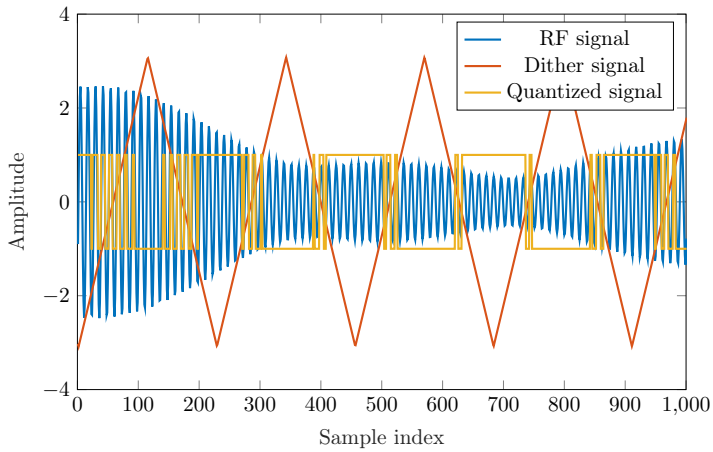

(a) Input and output time-domain signals.

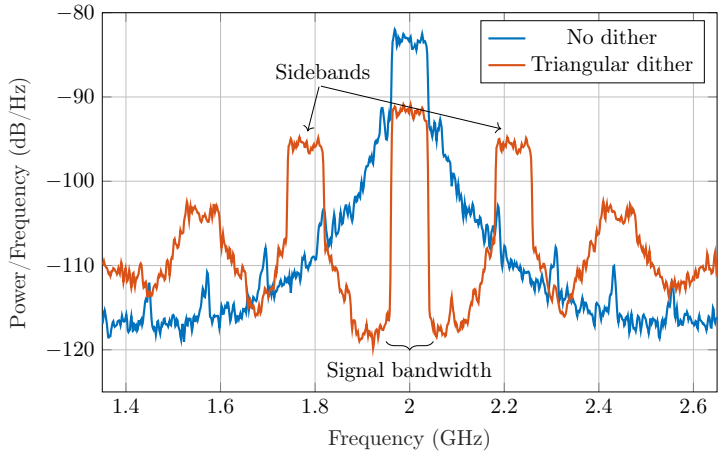

(b) Quantized signals in the frequency domain.

Figure 4.5. 1-Bit quantization of an RF signal dithered with a triangular wave.

eraging effect on the noise, spreading it over a wider frequency range. As a result, the noise floor is lowered, which improves the SNR. In the 1-bit radio-over-fiber fronthaul architecture, high sampling rates are essential for both uplink and downlink. On the downlink, the sampling rate must be sufficiently high to generate the carrier frequency and to enable the sigma-delta modulator to shape the quantization noise outside the signal bandwidth. For the uplink, as discussed in Papers A and B, heavy oversampling is necessary to whiten the quantization noise effectively.

CHAPTER 5

TDD D-MIMO Testbeds

We have now laid the foundation for the D-MIMO architecture that is analyzed and used in Papers A–C. This architecture enables signal transmission and reception between multiple base station antennas and several users, as described in Chapter 2, even when the base station antennas are arbitrarily placed. This is made possible by using the direct RF-sampling transceiver approach introduced in Chapter 3, which avoids synchronization of distributed LOs. To maintain low complexity and scalability, the system implements 1-bit radio-over-fiber as the fronthaul method, as presented in Chapter 4. These choices imply that the CU is responsible for all signal processing tasks, including digital up- and down-conversion. This introduces complexity in the CU, as it requires high sampling rates and increased data processing capabilities. In turn, this increases the computational burden and complicates the signal processing algorithms to handle vast amounts of data efficiently.

Although it requires perhaps the most simple RRHs, this architecture is not the only viable approach to implement D-MIMO. To complement our design choices and perhaps further motivate them, we shall in this chapter discuss other implementations that have successfully demonstrated multi-user D-MIMO.

5.1 MegaMIMO

The testbed presented in [47], which builds on the downlink implementation in [48], demonstrates a multi-user D-MIMO setup comprising four RRHs and four UEs. Each RRH is equipped with the programmable system-on-chip *ZedBoard* and the RF front-end *FMCOMMS2* from Analog Devices, facilitating digital signal processing within the RRH. Consequently, each RRH operates with its own LO, necessitating synchronization across nodes. This system achieves phase synchronization wirelessly, through a master-slave approach. The master RRH broadcasts a synchronization header, allowing all slave RRHs to estimate their relative phase offset, timing, and the frequency offset. This header also serves as a trigger for synchronized transmission across all nodes. It is shown in [47] that the throughput of the MegaMIMO testbed can scale linearly with the number of nodes, showcasing its potential for increasing capacity.

The complexity of the MegaMIMO architecture primarily lies in the synchronization required for each RRH. Advanced algorithms are essential to maintain synchronization among all RRHs, ensuring coherent signal processing. Despite these capabilities, the scalability of the system when the number of nodes significantly increases remains uncertain. As discussed in [17], wireless synchronization faces unavoidable scalability issues for certain topologies. Furthermore, the robustness of the system depends on the stability and reliability of the master RRH. To ensure a resilient network, redundant synchronization mechanisms should be explored.

5.2 Bi-Directional Sigma-Delta

The testbed detailed in [40] features a design that employs sigma-delta modulation for both uplink and downlink communications. This architecture uses thereby wired fronthaul. The RRHs are each built from the FPGA VCU108 and an in-house developed active antenna unit. The testbed is used to demonstrate multi-user measurements using a symmetrical setup with four UEs and four RRHs, reporting EVM performance that complies with the 3GPP requirements within a deployment area of approximately $1\,\mathrm{m} \times 2\,\mathrm{m}$. To enable and maintain phase-synchronized transmission among the RRHs, the system relies on the clock in the CU. In the downlink process, the architecture in-

volves sigma-delta modulation performed on the baseband signals at the CU. These modulated and precoded signals are transmitted via optical fiber to the RRHs. At each RRH, digital up-conversion is performed using a clock recovered from the incoming data stream. For the uplink, received signals are initially down-converted in the analog domain using the clock recovered in the downlink transmission. These signals are then sampled by an ADC. Once digitized, the samples undergo sigma-delta modulation before being sent to the CU.

The complexity of this system primarily lies in the RRH hardware and clock-recovery mechanisms. Sophisticated platforms and components are required to facilitate system-wide phase stability across the transceivers, sigma-delta modulation, and frequency conversion.

5.3 IF-over-Coaxial Cable for mm-Wave

In [49], a network deployment featuring 8 RRHs and 8 UEs within an 8 m × 7 m area is described. Each RRH incorporates a multiplexer, mixers, band-pass filters, and an eight-channel transceiver integrated complementary metal-oxide-semiconductor (CMOS) circuit, paired with 8 antenna elements. This integrated circuit includes transmit and receive amplifiers, phase shifters, and TDD switches. Communication between the CU and the RRHs is facilitated via coaxial cables, with signals transmitted and received at IF. Conversion between IF and RF occurs within the RRH, utilizing a clock signal supplied through the coaxial cable. The study examines the SNR measured at the UE in the downlink, offering a comparative analysis between D-MIMO and co-located MIMO deployments. The evaluation explores different configurations by varying the number of UEs and RRHs. Findings indicate that the D-MIMO deployment consistently delivers superior SNR compared to the co-located setup.

While demonstrating impressive capabilities, this testbed presents a limitation in the distance between the CU and the RRHs. To ensure accurate synchronization, the clock signal at each RRH must maintain high stability, which puts high requirements on the coaxial cables. However, coaxial cables are efficient only over short distances (in the order of 10 m), after which the signal quality and latency becomes deficient.

CHAPTER 6

Summary of Included Papers

This chapter provides a summary of the included papers.

6.1 Paper A

Lise Aabel, Sven Jacobsson, Mikael Coldrey, Frida Olofsson, Giuseppe Durisi, Christian Fager
A TDD Distributed MIMO Testbed Using a 1-Bit Radio-Over-Fiber Fronthaul Architecture
Published in IEEE Transactions on Microwave Theory and Techniques, vol. 72, no. 10, pp. 6140–6152, Oct. 2024.
 DOI: 10.1109/TMTT.2024.3389151 .

This paper introduces a D-MIMO testbed utilizing a 1-bit radio-over-fiber architecture for both uplink and downlink communications. The system features a central unit with 10 GS/s 1-bit converters connected via optical fibers to multiple remote radio heads. Experimental results demonstrate that despite 1-bit sampling, the system achieves low error-vector magnitude (EVM) in point-to-point and multi-user scenarios, including over-the-air transmissions

with reciprocity calibration and zero-forcing precoding. The paper also explores the system's capability to support OFDM waveforms and its resilience to interference, showcasing its potential for efficient, large-scale MIMO deployments.
Contributions: S. Jacobsson, G. Durisi and C. Fager proposed the system architecture. L. Aabel constructed the testbed, conducted the measurements and analysis, and wrote the paper. S. Jacobsson contributed to the signal processing. S. Jacobsson, G. Durisi, C. Fager, F. Olofsson and M. Coldrey supported the progress through continuous discussions.

6.2 Paper B

Anzhong Hu, **Lise Aabel**, Giuseppe Durisi, Sven Jacobsson, Mikael Coldrey, Christian Fager, Christoph Studer
EVM Analysis of Distributed Massive MIMO with 1-Bit Radio-over-Fiber Fronthaul
Published in IEEE Transactions on Communications,
vol. 72, no. 11, pp. 7342–7356, Nov. 2024.
 DOI: 10.1109/TCOMM.2024.3412769 .

This paper examines the uplink performance of the D-MIMO architecture presented in paper A. Remote access points (APs) are connected to a central processing unit via fiber-optic fronthaul carrying dithered, 1-bit quantized RF signals. The study investigates the tradeoff between spatial oversampling (number of APs) and temporal oversampling (sampling rate at the central processing unit) under fronthaul bandwidth constraints, aiming to optimize signal recovery from the 1-bit samples. Using EVM as a performance metric, the analysis provides insights into the optimal dither signal design and determines the minimum fronthaul rate needed for the system to outperform traditional co-located massive MIMO configurations.
Contributions: A. Hu, G. Durisi and S. Jacobsson proposed the problem. G. Durisi and A. Hu derived the asymptotic characterization. L. Aabel contributed to the system model and simulations. All authors engaged in discussions and analysis.

6.3 Paper C

Lise Aabel, Giuseppe Durisi, Mikael Coldrey, Frida Olofsson, Christian Fager
Insights on the Uplink Operation of a 1-bit Radio-over-Fiber Architecture in Multi-User D-MIMO Communication
Submitted to IEEE Transactions on Microwave Theory and Techniques
.

This paper introduces a testbed and hardware model to investigate multi-user configurations in a distributed MIMO network using a 1-bit radio-over-fiber architecture. The study evaluates both uplink and downlink error-vector magnitude (EVM) performance in various deployment setups. Results show that distributed deployments are more energy-efficient and deliver better EVM performance compared to co-located configurations. The research highlights that the 1-bit architecture is more affected by path-loss variations in the uplink than high-precision systems, but simulation results suggest that UE transmit power control can mitigate this sensitivity.
Contributions: L. Aabel contributed to formulating the research questions, designed and constructed the testbed, conducted all measurements and simulations, and wrote the paper. G. Durisi, M. Coldrey, F. Olofsson and C. Fager contributed through discussions and analysis.

CHAPTER 7

Concluding Remarks and Future Work

In this thesis, we investigate a multi-user D-MIMO architecture, that is based on 1-bit radio-over-fiber fronthaul. The investigations involve testbed implementation and demonstration of real-world D-MIMO scenarios. Our research shows that this architecture can be used for reciprocity-based coherent joint transmission from geographically dispersed RRHs. Paper A focuses on the hardware design and system implementation aspects, while Paper B offers theoretical guidelines for deploying the system efficiently under limited fronthaul resources. Paper C extends the measurement evaluation to larger multi-user scenarios, assessing overall system performance. Together, these works provide a solid foundation for understanding both the capabilities and limitations of the 1-bit radio-over-fiber architecture.

In a broader perspective, the findings of this thesis contribute to the larger effort in advancing the next generation of wireless communication networks. By demonstrating the practical feasibility of a 1-bit radio-over-fiber fronthaul for coherent joint transmission, this research addresses a critical challenge in enabling scalable, cost-effective, and power-efficient network deployments. The combination of hardware prototyping, theoretical deployment strategies, and large-scale performance evaluations forms a comprehensive pathway from

concept to practice. To further strengthen the research in this area, there are many interesting topics to investigate.

For example, algorithm development is required to implement reciprocity calibration over large signal bandwidth. Only then can the testbed be utilized for reciprocity-based coherent joint transmission. This involves development of reciprocity calibration algorithms that efficiently compensate for the hardware differences between the uplink and downlink. By implementing such algorithms, the channel estimation phase would be significantly simplified in the D-MIMO deployment.

In the hardware domain, significant developments are required to enable real-time measurement capabilities. The testbeds employed in this thesis have relied exclusively on offline signal processing at the CU. While effective for controlled experiments, this approach imposes notable limitations: only static environments can be analyzed, and there is an inherent risk for channel aging. Transitioning to a real-time processing framework would enable measurement scenarios involving movement. By executing signal processing tasks directly on the FPGA and streamlining the data transfer, the computation time would decrease to support time-sensitive measurement campaigns. The architecture could then be used to investigate more complex propagation scenarios, and joint communication, localization, and sensing use-cases. Real-time processing involves moving signal processing tasks onto the FPGA, and streamlining data transfer to and from the FPGA. These advancements would allow the architecture to serve as a flexible platform for next-generation wireless research, bridging the gap between laboratory measuremnts and operational field trials.

Another interesting development of the architecture is to investigate extension to the most recent advances in SFP technology, such as the QSFP-DD module. This device implements pulse-amplitude modulation (PAM) modulation in the optical domain. By increasing the resolution of the quantizer from 1 bit to 2 bits or 3-bits, the signal distortion could be significantly reduced [50]. Such development to the architecture could improve the system overall performance.

References

[1] Ericsson AB, "Ericsson mobility report", Tech. Rep., Nov. 2024.

[2] T. L. Marzetta, E. G. Larsson, H. Yang, and H. Q. Ngo, *Fundamentals of massive MIMO*. Cambridge Univ. Press, 2016.

[3] D. Tse and P. Viswanath, *Fundamentals of Wireless Communication*. Cambridge Univ. Press, 2005.

[4] Ö. T. Demir, E. Björnson, and L. Sanguinetti, *Foundations of user-centric cell-free massive MIMO*. Now Publisher, Foundations and Trends in Signal Processing, 2021.

[5] A. Goldsmith, *Wireless communications*. Cambridge Univ. Press, 2005.

[6] S. Zhou, M. Zhao, X. Xu, J. Wang, and Y. Yao, "Distributed wireless communication system: A new architecture for future public wireless access", *IEEE Commun. Mag.*, vol. 41, no. 3, pp. 108–113, Mar. 2003.

[7] 3GPP, *Coordinated multi-point operation for LTE physical layer aspects*, TR 36.819 version 11.2.0 Rel. 11, 2013.

[8] J. Mocerino, "5G backhaul/fronthaul opportunities and challenges", Fujitsu Network Communications, Tech. Rep., 2019.

[9] Common Public Radio Interface, *eCPRI interface specification*, V2.0, 2019.

[10] O. Andersson, *Functional splits: The foundation of an open 5G RAN*, [Online]. Available: `https://www.5gtechnologyworld.com/functional-splits-the-foundation-of-an-open-5g-ran/`.

[11] P. Luong, F. Gagnon, C. Despins, and L.-N. Tran, "Optimal joint remote radio head selection and beamforming design for limited fronthaul C-RAN", *IEEE Trans. Signal Process.*, vol. 65, no. 21, pp. 5605–5620, Nov. 2017.

[12] D. Rajan and S. Gray, "Transmit diversity schemes for CDMA-2000", in *IEEE Wireless Commun. Netw. Conf.*, vol. 2, New Orleans, LA, USA, Aug. 1999, pp. 669–673.

[13] M. Pelgrom, *Analog-to-Digital Conversion*, 3rd ed. Springer Nature, 2017.

[14] S. Mulleti, T. Zirtiloglu, A. Tan, R. T. Yazicigil, and Y. C. Eldar, "Power-efficient sampling: Towards low-power analog-to-digital converters", *IEEE Signal Process. Mag.*, vol. 42, no. 2, pp. 106–125, Mar. 2025.

[15] B. Murmann, *ADC Performance Survey 1997-2025*, [Online]. Available: `https://github.com/bmurmann/ADC-survey`.

[16] E. Rubiola, *Phase Noise and Frequency Stability in Oscillators*. Cambridge Univ. Press, 2008.

[17] E. G. Larsson, "Massive synchrony in distributed antenna systems", *IEEE Trans. Signal Process.*, vol. 72, pp. 855–866, 2024.

[18] Hexa-X-II, "Deliverable D4.5, Final results of 6G radio key enablers", Tech. Rep., Feb. 2025.

[19] H. Yuan, S. Jin, C.-K. Wen, and K.-K. Wong, "The distributed MIMO scenario: Can ideal ADCs be replaced by low-resolution ADCs?", *IEEE Wireless Commun. Lett.*, vol. 6, no. 4, pp. 470–473, Aug. 2017.

[20] S. Jacobsson, L. Aabel, M. Coldrey, *et al.*, "Massive MU-MIMO-OFDM uplink with direct RF-sampling and 1-bit ADCs", in *Proc. IEEE Global Telecommun. Conf. (GLOBECOM)*, Waikoloa, HI, USA, Dec. 2019.

[21] D. Siafarikas and J. L. Volakis, "Toward direct RF sampling: Implications for digital communications", *IEEE Microw. Mag.*, vol. 21, no. 9, pp. 43–52, Aug. 2020.

[22] S. Henthorn, R. Mohammadkhani, T. O'Farrell, and K. L. Ford, "The effect of ADC resolution on concurrent, multiband, direct RF sampling receivers", in *Proc. IEEE Global Telecommun. Conf. (GLOBECOM)*, Madrid, Spain, Dec. 2021.

[23] A. Nirmalathas, P. A. Gamage, C. Lim, D. Novak, R. Waterhouse, and Y. Yang, "Digitized RF transmission over fiber", *IEEE Microw. Mag.*, vol. 10, no. 4, pp. 75–81, Jun. 2009.

[24] L. Breyne, G. Torfs, X. Yin, P. Demeester, and J. Bauwelinck, "Comparison between analog radio-over-fiber and sigma delta modulated radio-over-fiber", *IEEE Photon. Technol. Lett.*, vol. 29, no. 21, pp. 1808–1811, Nov. 2017.

[25] F. Olofsson, L. Aabel, M. Karlsson, and C. Fager, "Comparison of transmitter nonlinearity impairments in externally modulated sigma-delta-over-fiber vs analog radio-over-fiber links", in *Opt. Fiber Commun. Conf. Exhibit. (OFC)*, San Diego, CA, USA, Mar. 2022.

[26] R. Puerta, M. Han, M. Joharifar, *et al.*, "NR conformance testing of analog radio-over-LWIR FSO fronthaul link for 6G distributed MIMO networks", in *Opt. Fiber Commun. Conf. Exhibit. (OFC)*, San Diego, CA, USA, Mar. 2023.

[27] D. Perez-Galacho, D. Sartiano, and S. Sales, "Analog radio over fiber links for future 5G radio access networks", in *Int. Conf. Transparent Opt. Netw. (ICTON)*, Angers, France, Jul. 2019.

[28] V. A. Thomas, M. El-Hajjar, and L. Hanzo, "Performance improvement and cost reduction techniques for radio over fiber communications", *IEEE Commun. Surv. Tut.*, vol. 17, no. 2, pp. 627–670, 2015.

[29] L. M. Pessoa, J. S. Tavares, D. Coelho, and H. M. Salgado, "Experimental evaluation of digitized fiber-wireless system employing sigma delta modulation", *Opt. Soc. Am.*, vol. 22, no. 14, Jul. 2014.

[30] H. Inose, Y. Yasuda, and J. Murakami, "A telemetering system by code modulation - Δ-Σ modulation", *IRE Trans. Space Electron. Telemetry*, vol. SET-8, no. 3, pp. 204–209, 1962.

[31] S. Pavan, R. Schreier, and G. C. Temes, *Understanding Delta-Sigma Data Converters*, 2nd ed. John Wiley & Sons, 2017.

[32] A. Prata, A. S. Oliveira, and N. B. Carvalho, "All-digital flexible uplink remote radio head for C-RAN", in *IEEE MTT-S Int. Microw. Symp.*, San Francisco, CA, USA, May 2016.

[33] I. C. Sezgin, L. Aabel, S. Jacobsson, G. Durisi, Z. S. He, and C. Fager, "All-digital, radio-over-fiber, communication link architecture for time-division duplex distributed antenna systems", *J. Lightw. Technol.*, vol. 39, no. 9, pp. 2769–2779, May 2021.

[34] L. Aabel, G. Durisi, I. C. Sezgin, S. Jacobsson, C. Fager, and M. Coldrey, "Distributed massive MIMO via all-digital radio over fiber", in *Asilomar Conf. Signals, Syst., Comput.*, Pacific Grove, CA, USA, Jun. 2020.

[35] L. Aabel, S. Jacobsson, M. Coldrey, F. Olofsson, G. Durisi, and C. Fager, "A TDD distributed MIMO testbed using a 1-bit radio-over-fiber fronthaul architecture", *IEEE Trans. Microw. Theory Techn.*, vol. 72, no. 10, pp. 6140–6152, Oct. 2024.

[36] J. M. de la Rosa, "Bandpass sigma–delta modulation: The path toward RF-to-digital conversion in software-defined radio", *Chips*, 2023.

[37] R. F. Cordeiro, A. Prata, A. S. Oliveira, J. M. Vieira, and N. B. De Carvalho, "Agile all-digital RF transceiver implemented in FPGA", *IEEE Trans. Microw. Theory Techn.*, vol. 65, no. 11, pp. 4229–4240, Nov. 2017.

[38] S. S. Pereira, L. F. Almeida, D. C. Dinis, A. S. R. Oliveira, P. P. Monteiro, and N. B. Carvalho, "Frequency-agile real-time all-digital transmitter with 1 GHz of bandwidth", *IEEE Trans. Circuits Syst. II, Exp. Briefs*, vol. 70, no. 8, pp. 2844–2848, Aug. 2023.

[39] T. Maehata and N. Suematsu, "Time division multiplexing for 1-bit bandpass delta-sigma modulator", *TechRxiv*, May 2024.

[40] A. Vandierendonck, K.-L. Chiu, C. Meysmans, *et al.*, "A bi-directional distributed multi-user MIMO testbed using digital sigma-delta-over-fiber", *J. Lightw. Technol.*, vol. 43, no. 4, pp. 1595–1603, Feb. 2025.

[41] N. V. Silva, A. S. R. Oliveira, U. Gustavsson, and N. B. Carvalho, "A novel all-digital multichannel multimode RF transmitter using delta-sigma modulation", *IEEE Microw. Wirel. Compon. Lett.*, vol. 12, no. 3, pp. 156–158, Mar. 2012.

[42] L. Schuchman, "Dither signals and their effect on quantization noise", *IEEE Trans. Commun. Technol.*, vol. 12, no. 4, pp. 162–165, 1964.

[43] J. Sun, "Pulse-width modulation", in *Dynamics and control of switched electronic systems*, Springer, 2012.

[44] S. Y. Suh, "Pulse width modulation for analog fiber-optic communications", *J. Lightw. Technol.*, vol. 5, pp. 102–112, Jan. 1987.

[45] D. G. Holmes and T. A. Lipo, *Pulse Width Modulation for Power Converters: Principles and Practice*. John Wiley & Sons, 2003.

[46] H. du Toit Mouton, B. McGrath, D. Grahame Holmes, and R. H. Wilkinson, "One-dimensional spectral analysis of complex PWM waveforms using superposition", *IEEE Trans. Power Electron.*, vol. 29, no. 12, pp. 6762–6778, Dec. 2014.

[47] E. Hamed, H. Rahul, M. Abdelghany, and D. Katabi, "Real-time Distributed MIMO Systems", in *Proc. ACM SIGCOMM Conf.*, Florianópolis, Brazil, Aug. 2016.

[48] H. Rahul, S. Kumar, and D. Katabi, "MegaMIMO: Scaling wireless capacity with user demands", in *Proc. ACM SIGCOMM Conf.*, Helsinki, Finland, Aug. 2012.

[49] T. Kaneko, T. Kuwabara, N. Tawa, and Y. Maruta, "Bit efficiency of distributed- and collocated-massive MIMO base station systems in OTA measurement and simulation", *Intern. J. Microw. Wireless Technol.*, vol. 17, no. 2, pp. 234–245, Dec. 2024.

[50] J. D. Domingues, S. S. Pereira, L. F. Almeida, H. S. Silva, A. S. R. Oliveira, and N. B. Carvalho, "Agile and wideband PAM4-based all-digital receiver", in *Radio Wireless Symp.*, San Juan, PR, USA, Jan. 2025.